J. Fluid Mech. (1967), *vol.* 30, *part* 3, *pp.* 479–487
Printed in Great Britain

The velocity distribution function within a shock wave

By G. A. BIRD
Department of Aeronautical Engineering, University of Sydney

(Received 21 March 1967)

The structure of normal shock waves in a gas composed of rigid sphere molecules is investigated by numerical experiments with a simulated gas on a digital computer. The non-equilibrium between the temperatures based on the longitudinal and lateral velocity components is studied and the results compared with the theory of Yen (1966). Details of the velocity distribution function are presented for a shock of Mach number 10. The distribution functions for both the longitudinal and lateral velocity components are plotted for a number of locations in the shock profile and are compared with the equilibrium distribution.

1. Introduction

Problems in gas dynamics which involve significant changes in flow properties over distances of the order of the mean free path are amenable to a direct simulation Monte Carlo method which has been developed by the author. Although the shock structure problem has already been treated (Bird 1965), this was in the early stages of the development of the method, and a number of significant modifications have since been made to it. These refinements have reduced the computing requirements by more than an order of magnitude so that the method can now be readily applied on any modern medium- to large-sized computer. In the case of the shock wave problem, this increased speed has not only led to an increase in the accuracy of the shock profile determination, but has enabled the details of the velocity distribution function to be obtained.

The approach is to conduct numerical experiments with a model gas on the computer. The real gas is simulated by the order of a thousand rigid sphere molecules which may be thought of as a representative sample of the many billions of molecules in a real shock wave. The positions and the velocity components of the simulated molecules are stored in the computer and typical collisions are computed among them as a time parameter is advanced. The desired steady flow is obtained as the large time solution of an unsteady flow set up by the application of appropriate boundary conditions. In the present case, the computation of collisions starts at zero time, the molecules having been set up as a uniform stream at the required upstream Mach number. A specularly reflecting plane piston is inserted into this flow at zero time with its face normal to the flow direction. The velocity of the piston is set equal to velocity downstream of a steady normal shock wave at the stream Mach number. The transient effects due to the instantaneous application of the boundary conditions die out, leaving a steady normal shock wave in the flow. It is interesting to note that the point of inflexion in the density profile of this shock is always located at the point of insertion of the piston.

2. Description of method

The flow is in the positive x direction and the simulated region extends from $-b\lambda_1$ to $+b\lambda_1$, where λ_1 is the upstream mean free path and b is sufficiently large to locate the boundaries well outside a shock wave centred at the origin. This region is divided into a number of cells which are made sufficiently narrow for the change in flow properties from one side of each cell to the other to be small. Since the problem is one-dimensional, it is necessary to store only the x position co-ordinate for each simulated molecule. The three velocity components and the cell number are also stored.

The first step is to generate the initial, or zero time, configuration of simulated molecules. The molecules are distributed uniformly between the upstream boundary at $x = -b\lambda_1$ and the origin. This means that all locations in this range are equally likely for each molecule and the x co-ordinate of the nth molecule, x_n, is obtained by generating a random number r and setting

$$x_n = -rb\lambda_1.$$

The sequence of random numbers is rectangularly distributed between 0 and 1 and is used in a number of procedures throughout the program. The velocity components are those appropriate to a gas in Maxwellian equilibrium and with a stream velocity in the x direction such that its Mach number is equal to the desired shock Mach number M_s. The probability of an individual peculiar velocity component having a value u times the most probable molecular speed at the free-stream temperature is proportional to $\exp(-u^2)$. The ratio of this probability to the maximum value of the probability (which occurs for $u = 0$) is also equal to $\exp(-u^2)$. The required distribution for each set of peculiar velocities may therefore be obtained through the general procedure for probabilistic variables (Bird 1966).

The molecules are then allowed to move and to collide among themselves. The two processes are uncoupled by computing collisions appropriate to a time interval Δt_m and by then moving the molecules through distances appropriate to Δt_m and their instantaneous velocities. The distortion produced in the molecular paths by this approximation is small as long as Δt_m is small compared with the mean time between collisions. This time will be of the order of $(\pi\sigma^2 N v_{rm})^{-1}$ where N is the number density, σ is the molecular diameter and v_{rm} is the mean relative velocity of the collision pairs. A value of Δt_m is chosen much less than an estimated mean time between collisions and is verified by recording the actual mean collision time during the running of the program.

Since the change in flow properties over the width of each cell is small, the molecules in a cell at any instant may be regarded as a sample of the molecules at the location of the cell. The relative location of the various molecules within the cell can then be disregarded and the collision probability of a particular pair of molecules within the cell depends only on their relative velocity.† A pair of molecules is chosen at random from those within the cell under consideration and is retained or rejected in such a way that the probability of retention is proportional to the relative velocity v_r. When a pair is retained, a typical collision is computed between the two molecules and the new velocity components are stored in place of the old ones. The random selection of impact parameters is particularly simple for rigid sphere molecules since all directions for the new relative velocity vector are equally probable. For each collision, the time counter for this cell is advanced by

$$\Delta t = (2/N_c) \times (\pi\sigma^2 N v_r)^{-1},$$

where N_c is the actual number of molecules in the cell. Collisions are computed in the cell until the time counter has advanced through Δt_m. When this procedure has been carried out for every cell, the overall time is advanced through Δt_m and the molecules are moved through appropriate distances.

The set of molecules in each cell will change as the molecules are moved and appropriate conditions must be applied at the boundaries of the region being simulated. The upstream boundary at $x = -b\lambda_1$ is treated as a source of molecules with velocity components representative of the downstream moving molecules in the equilibrium free stream. The distribution function for molecules crossing a surface is different from that for those within a volume. For a velocity component in the stream direction of u times the most probable thermal speed, the ratio of the probability to the maximum probability is

$$\frac{2(u+U)}{U+(U^2+2)^{\frac{1}{2}}} \exp\left[\tfrac{1}{2}+\tfrac{1}{2}U\{U-(U^2+2)^{\frac{1}{2}}\}-u^2\right],$$

where U is the ratio of the stream velocity to the most probable thermal speed. Consideration is restricted to positive values of $U+u$ since only the downstream moving molecules are generated. Any molecule which moves back upstream across this boundary is regarded as being 'lost' and is removed from the store. The downstream boundary is a specularly reflecting wall which at zero time starts moving from the origin with velocity U_p which is related to M_s and the upstream speed of sound a_1 by

$$\frac{U_p}{a_1} = \frac{3}{4M_s}\left(1+\frac{M_s^2}{3}\right).$$

After the piston passes beyond the downstream limit of the simulated region at $x = b\lambda_1$, the piston location is restored to $x = b\lambda_1$ at the end of each time step. The molecules which finish beyond $x = b\lambda_1$ during the time step are removed from the calculation.

The time required for the piston to reach the downstream boundary approximates the time required to set up the steady shock wave profile. The required flow properties can then be sampled. The statistical scatter can be reduced by

---

† The reasoning behind the procedure adopted to choose the second molecule for a collision pair in the earlier treatment (Bird 1965) of the shock wave problem was incorrect. The actual procedure used in later work on two-dimensional steady flows (Bird 1966) was also incorrect.

the averaging of a number of samplings which are separated by the time interval Δt_s. This interval should exceed the time required for the slowest section of the flow to traverse one cell.

The key to the simulation is the procedure which selects the molecules in a collision pair according to the correct probability and then advances the time parameter by the appropriate amount for each individual collision. In this way, an appropriate set of collisions is computed for any distribution function of molecular velocities. Only two approximations are made. The first is the uncoupling of the molecular collisions and motion and this becomes exact as Δt_m tends to zero. The second is the assumption of uniform properties across the cell and this disappears as the cell width tends to zero. There has not been any sign of instabilities induced in the flow as a result of the statistical fluctuations, even though runs have been made with as few as six simulated molecules in each cell.

The computations were carried out on an English Electric KDF-9 computer, a typical run lasting approximately 20 min.

3. Results

Typical results for the density profile through the shock wave are shown in figures 1 and 2. The agreement between the Monte Carlo result and the Navier–Stokes solution (Gilbarg & Paolucci 1953) is well within the expected statistical scatter for a shock Mach number of 1·5. As expected, the thickness increases beyond the Navier–Stokes value as the shock Mach number increases and figure 2 indicates that, at $M_s = 10$, it is also slightly greater than the Mott-Smith thickness (Mott-Smith 1951). The most critical assumption made in the method is that implied by the choice of the second molecule in a collision pair from anywhere within the cell. The computation for the $M_s = 10$ case was therefore carried out for a number of cell widths. The results in figure 2 show that there is little systematic change in the shock profile with cell width even when the latter becomes almost comparable with the width of the wave.

An indication of the degree of non-equilibrium within the shock is given by the difference between the temperature T_x associated with the longitudinal components of the thermal velocities and the temperature T_n associated with the lateral components. These quantities were therefore sampled in addition to the overall temperature T. Typical results are shown in figures 3 and 4 for shock Mach numbers of 3 and 10 respectively. These results are in good agreement with the theory of Yen (1966) which predicts a maximum longitudinal temperature of 4·28 for $M_s = 3$ and 42·1 for $M_s = 10$.

The velocity distribution function was sampled for the shock of Mach number 10 and is shown in figures 6 and 7 for each of the five locations marked on the velocity profile in figure 5. In plotting the distribution function f_x for the longitudinal velocities in figure 6, the peculiar velocity component v_x has been non-dimensionalized by dividing it by $(2RT_x)^{\frac{1}{2}}$ where R is the gas constant. Similarly, in figure 7, the lateral peculiar velocity component v_n has been divided by $(2RT_n)^{\frac{1}{2}}$. The values of T_x and T_n at the five locations are shown in figure 4. The equilibrium (Maxwellian) distribution function is included for comparison as a solid line. Broken lines have been drawn through the points for locations B, C and D only as an aid to clarity, since the statistical scatter is such that some of the minor variations in these curves may not be significant.

Location A is situated upstream of the shock wave and both longitudinal and lateral distribution functions agree, within the statistical scatter, with the

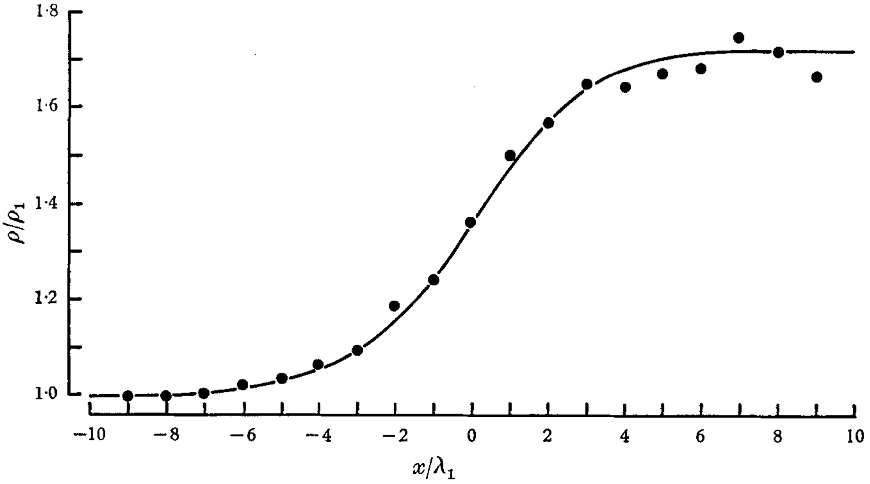

FIGURE 1. Density profile through shock of Mach number 1·5. ●, model gas; ——, Navier–Stokes.

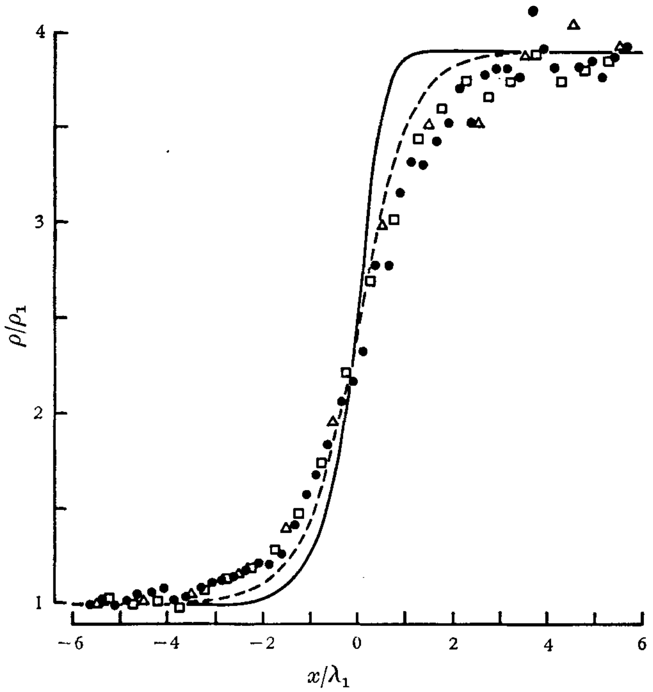

FIGURE 2. Density profile through shock of Mach number 10. Model gas with cell width ●, $\frac{1}{4}\lambda_1$; □, $\frac{1}{2}\lambda_1$; △, λ_1: ——, Navier–Stokes; – – –, Mott-Smith.

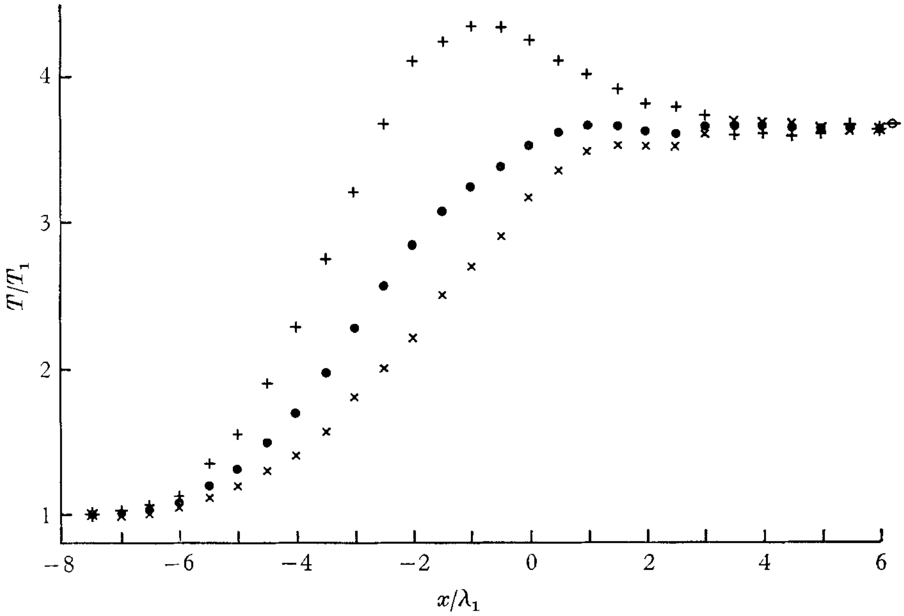

FIGURE 3. Temperature non-equilibrium in shock of Mach number 3. +, longitudinal temperature ratio; ×, lateral temperature ratio; ●, overall temperature ratio; ⊖, Rankine–Hugoniot downstream temperature.

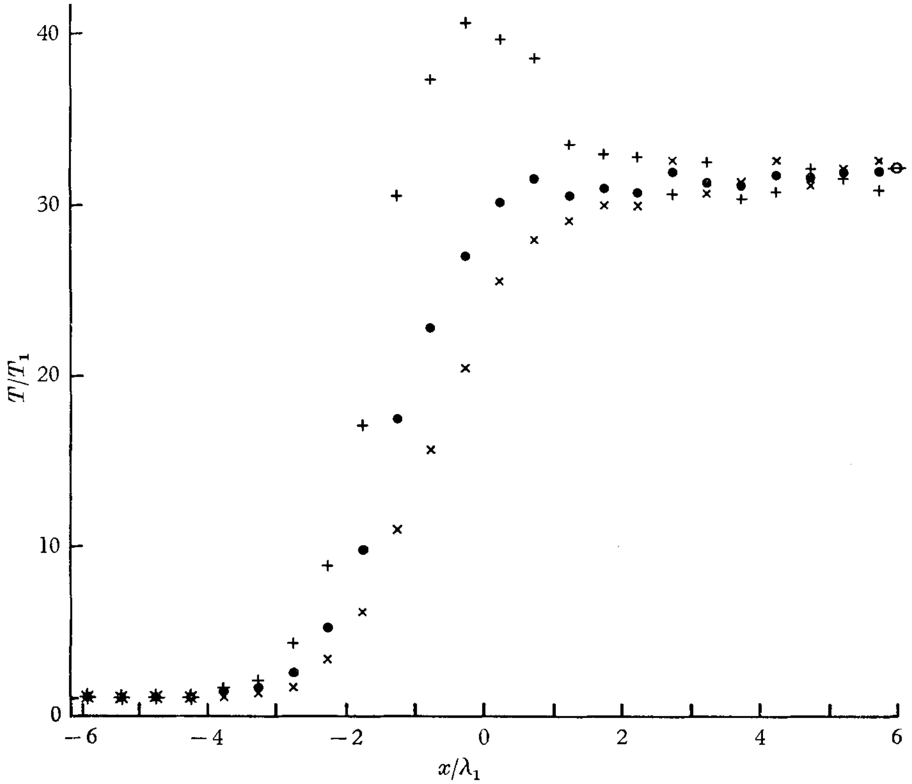

FIGURE 4. Temperature non-equilibrium in shock of Mach number 10. +, longitudinal temperature ratio; ×, lateral temperature ratio; ●, overall temperature ratio; ⊖, Rankine–Hugoniot downstream temperature.

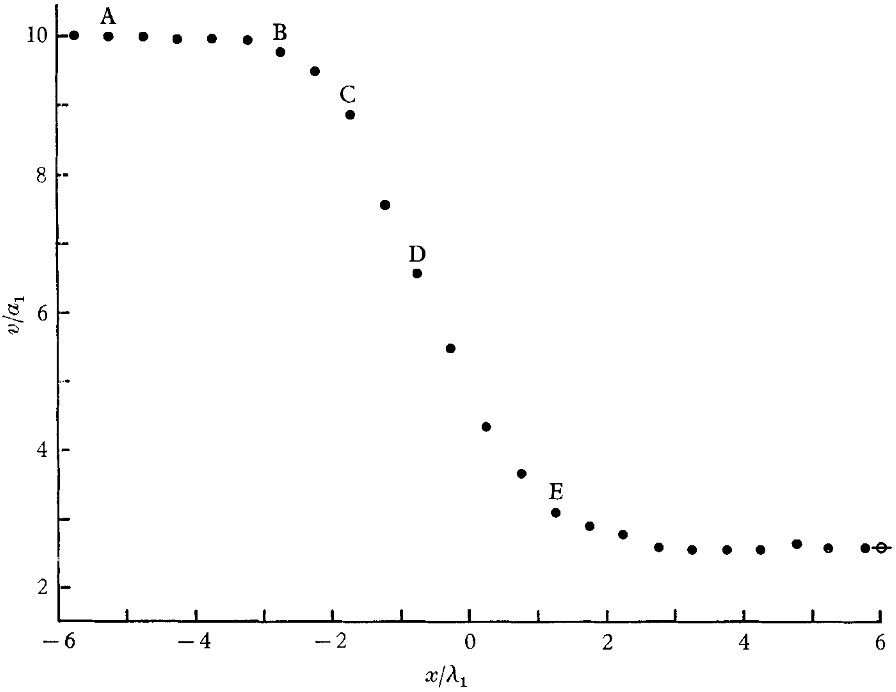

FIGURE 5. Velocity profile through shock of Mach number 10 showing locations at which the distribution function was sampled.

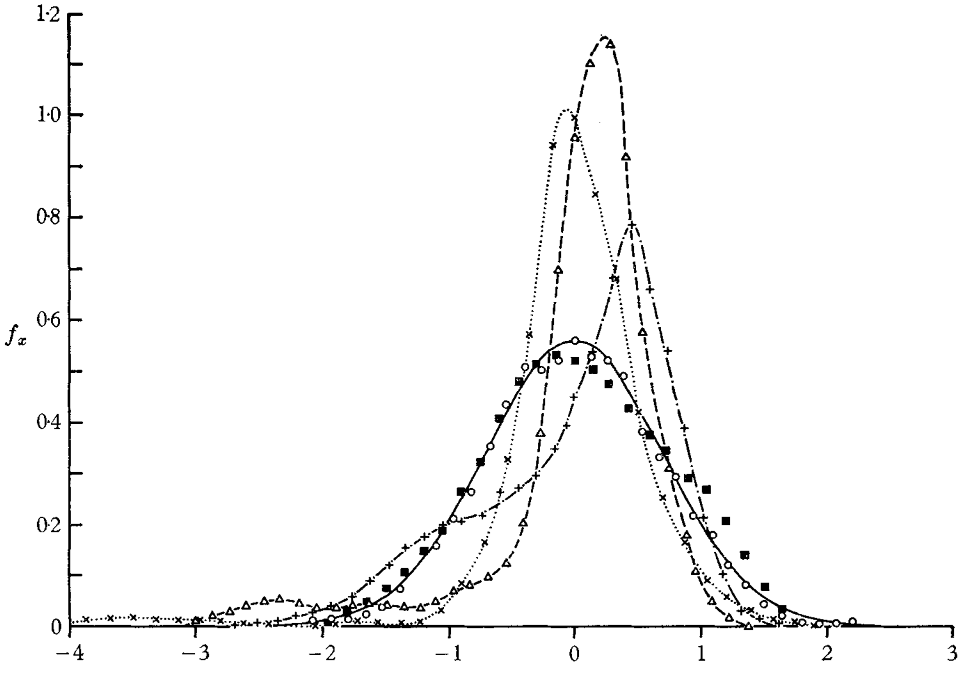

FIGURE 6. Longitudinal velocity distribution function for shock of Mach number 10. ○, location A; ×, B; △, C; +, D; ■, E: ——, Maxwellian distribution.

equilibrium distribution. In fact, the departure of these points from the equilibrium distribution gives an indication of the probable scatter in the other distributions.

The second location B is situated just within the shock wave profile where the velocity is barely affected but where the longitudinal temperature ratio has risen to approximately 4·2. The distribution function shows that this temperature rise is almost entirely due to a long 'tail' of molecules with large negative longitudinal peculiar velocity components. Since the velocity is positive in the direction of motion, this tail represents those few molecules that have been appreciably slowed by collisions in this region of the wave. The lateral distribution function also exhibits a high-speed tail at this location, but, since the lateral temperature

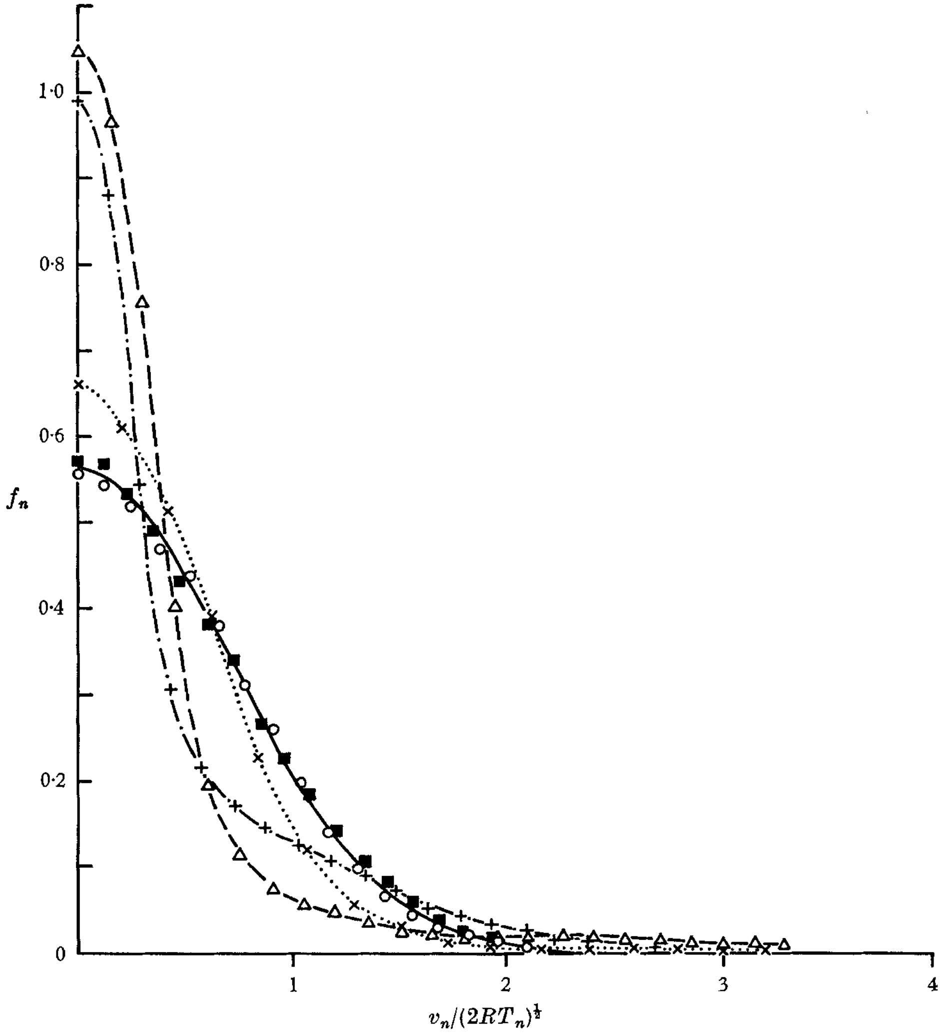

FIGURE 7. Lateral velocity distribution function for shock of Mach number 10. ○, location A; ×, B; △, C; +; D; ■, E: ——, Maxwellian distribution.

ratio is only 1·6, the magnitude of these peculiar velocity components is much smaller.

The third location C is situated well within the wave and the negative tail of the longitudinal distribution function is thicker and shorter. However, the longitudinal temperature ratio now exceeds 17 so that the magnitude of the peculiar velocities has increased. There is a marked asymmetry in the distribution function with the most probable velocity having a small positive value and a shallow second peak occurring on the negative side. The lateral distribution function now shows a more marked high speed tail and a higher central maximum.

At the centre of the wave where location D is situated, the distribution functions are showing a tendency to return to the equilibrium shape. This is most marked with the lateral function and the longitudinal function remains asymmetric with the most probable velocity shifted even further to the positive side. Finally, while the location E is situated well within the wave at a point where the lateral and longitudinal temperatures have not reached equilibrium, the distribution functions have returned almost to the equilibrium shape.

This research was sponsored by the Air Force Office of Scientific Research, Office of Aerospace Research, United States Air Force, under Grant AF-AFOSR-915-66.

REFERENCES

Bird, G. A. 1965 *Rarefied Gas Dynamics* (Ed. de Leeuw), p. 216. New York: Academic Press.

Bird, G. A. 1966 *AIAA J.* **4**, 55.

Gilbarg, D. & Paolucci, D. 1953 *J. Rat. Mech. Anal.* **2**, 617.

Mott-Smith, H. M. 1951 *Phys. Rev.* **82**, 885.

Yen, S-M. 1966 *Phys. Fluids*, **9**, 1417.